

LANDAU MODEL FOR UNIAXIAL SYSTEMS WITH COMPLEX ORDER PARAMETER

M. Latković and A. Bjeliš

*Department of Theoretical Physics, Faculty of Science
University of Zagreb, P.O.B. 162, 10001 Zagreb, Croatia*

We study the Landau model for uniaxial incommensurate-commensurate systems of the I class by keeping Umklapp terms of third and fourth order in the expansion of the free energy. It applies to systems in which the soft mode minimum lies between the corresponding commensurate wave numbers. The minimization of the Landau functional leads to the sine-Gordon equation with two nonlinear terms, equivalent to the equation of motion for the well-known classical mechanical problem of two mixing resonances. We calculate the average free energies for periodic, quasiperiodic and chaotic solutions of this equation, and show that in the regime of finite strengths of Umklapp terms only periodic solutions are absolute minima of the free energy, so that the phase diagram contains only commensurate configurations. The phase transitions between neighboring configurations are of the first order, and the wave number of ordering goes through harmless staircase with a finite number of steps. These results are the basis for the interpretation of phase diagrams for some materials from the I class of incommensurate-commensurate systems, in particular of those for A_2BX_4 and BCCD compounds. Also, we argue that chaotic barriers which separate metastable periodic solutions represent an intrinsic mechanism for observed memory effects and thermal hystereses.

64.70.Rh, 64.60.-i

I. INTRODUCTION

Usual treatments of uniaxial incommensurate-commensurate (IC-C) phase transitions are based either on microscopic models with competing interactions or on phenomenological Landau theories. The relevant reviews can be found in Refs.^{1,2}. The well-known example of the former is the Frenkel-Kontorova (FK) model^{3,4}, in which the wave number of ordering goes through the devil's staircase sequence of second order phase transitions³. In the regime of weak interactions the FK model can be continued, and so reduced to the exactly solvable (i. e. integrable) sine-Gordon model⁴. The solutions which then participate in the phase diagram are phase soliton lattices, i. e. commensurate regions separated by so called discommensurations⁵. The phase transition to the commensurate state is of the second (continuous) order, and the devil's staircase variation of the wave number is replaced by its simple continuous dependence on the control parameter.

The phenomenological Landau theory, another usual approach to the IC-C transitions, starts from the expansion of the thermodynamic potential in terms of the order parameter, relied on the symmetry requirement by which the order parameter is defined through one of the irreducible representations of the symmetry group of the normal phase. E. g., for structural phase transitions the order parameter is defined as a set of normal coordinates of the soft mode^{6,7}. Generally the minimum frequency of this soft mode may be located at an arbitrary point (i. e. star of wave vectors) in the first Brillouin zone. The simplest irreducible representation for an uniaxial ordering is then two-dimensional. The corresponding basic ("minimal") form of the Landau expansion comprises, besides the leading normal terms, one, presumably the strongest, Umklapp term allowed by symmetry. This term favors a commensurate ordering and is responsible for the lock-in transition from the incommensurate ordering favored by the elastic term. Minimization of the Landau functional again leads, after neglecting the space variations of the order parameter amplitude⁵, to the sine-Gordon equation^{8,9}, i. e. to the phase diagram equal to that of the FK model after the space continuation.

The above approaches predict either a dense sequence of second order phase transitions (devil's staircase in the FK model) or an isolated transition of the same type (Landau theory). Both possibilities are indeed close to the observations of IC-C transitions in some materials^{10,11}. A majority of materials however exhibits a more complex behavior comprising one or more first order phase transitions, memory effects, wide ("global") hystereses, finite density of solitons at the very IC-C transition, etc (for a review see e. g. Ref.¹¹). It is usually difficult to decide solely from the experimental observations, even for the most carefully prepared samples, whether such effects are of purely intrinsic or of some extrinsic origin. From the theoretical side, they cannot be explained within either of above approaches without extending the models. So far this problem was mainly considered by taking primarily into account some extrinsic agents, like external fields (e. g. electric field in ferroelectric materials), pinning centers, fixed or mobile defects, additional external periodic potentials with a periodicities different from that already present in the model), etc.

Another, more intricate possibility is that of intrinsic sources and mechanisms as the potential explanations for the afore mentioned phenomena¹². In this respect the central question is the following; what are the simplest intrinsic extensions of the above basic approaches which lead to phase diagrams with a finite sequence of first order transitions (i. e. harmless staircase¹³), and thus offer an inherent explanation for global hystereses and corresponding phenomena.

The attempts in this direction were more successful in the realm of discrete models. The examples are models which include couplings between next nearest neighbors, like so-called DIFFOUR model¹⁴, axial next-nearest neighbor Ising (ANNNI) model^{15,16}, as well as various extensions¹⁷⁻¹⁹, and models with two spin-like variables per site like those of Chen and Walker²⁰ and Janssen²¹. Both types of extensions were aimed mostly towards the interpretation of the phase diagrams observed in the family of A_2BX_4 compounds.

On the other hand, the attempts within Landau models were based on the formal inclusion of more and more Umklapp terms (i. e. stars of wave vectors) into the basic models for the classes I^{22-24} and II^{25-27} of IC-C systems. From one side, the relevance of the Umklapp terms of high orders in the Landau expansion can be hardly justified on the physical grounds. Also, the ensuing analyses took into account only sinusoidal modulations, which, as the present study shows, is a too crude approximation for the determination of phase diagrams with harmless staircase, as well as for the interpretation of accompanying hysteretic effects.

In contrast to such approaches, we propose in the present work a simple, physically well justified, extension of the basic Landau model for the class I, which is still framed within a "minimal" free energy expansion for a single star of wave vectors. The phase diagram which emerges from our model is characterized by a harmless staircase and first order transitions between highly nonsinusoidal configurations with different periods. Furthermore, a closer examination of configurations that participate in the phase diagram, and also of those that are not thermodynamically favored, enable a plausible explanation of the memory and hysteresis effects as the intrinsic (or at least semi-intrinsic) properties of IC-C systems.

Our considerations are based on a sine-Gordon model with two Umklapp terms²⁸. This type of model is physically well-grounded whenever the Landau expansion contains terms which favor two different commensurabilities, that are of comparable strengths. The most interesting case is realized with Umklapp terms of third and fourth order, the lowest possible ones within the models with the Lifshitz invariant, appropriate for the so-called systems of the I class⁶ (the systems of the II class have lock-in transitions at the commensurabilities of order one and two, and are covered by essentially different type of Landau models^{29,30}).

The mean-field (saddle point) approximation for our Landau functional leads to the Euler-Lagrange (EL) equation which has the form of the double sine-Gordon equation. This is one of the most intensively studied nonintegrable problems in the contemporary classical mechanics³¹⁻³³. The corresponding phase portrait contains periodic, quasiperiodic and chaotic trajectories, the latter appearing only when *both* nonlinear terms in the Landau functional are finite. As the strength of nonlinear terms increases, the chaotic trajectories occupy larger and larger portion of the phase space, destroying gradually quasiperiodic Kolmogorov-Arnold-Moser (KAM) layers, and eventually allowing only for some isolated periodic trajectories. The latter are orbitally unstable and therefore are not realized within the scope of classical mechanics. However, we show that just this tiny subset of the phase space comprises local minima of the free energy functional, i. e. the solutions (configurations) which participate in the thermodynamic phase diagram. The question which then arises is analogous to that met in the analyses of the discrete models^{3,34}, i. e. are there thermodynamically stable configurations among other, quasiperiodic and chaotic, trajectories.

In order to analyze this additional, *thermodynamic*, aspect of the phase portrait, we calculate the average free energy for periodic, quasiperiodic and a representative set chaotic solutions of EL equation, with the aim to find, for given values of control parameters, those solutions that have the lowest value of the average free energy. We show that the chaotic configurations are never thermodynamically stable, in agreement with results obtained for some discrete models^{3,34}. The quasiperiodic configurations might be present in the phase diagram only when the Umklapp terms are weak enough, i. e. at temperatures slightly below the phase transition from the disordered to the incommensurate state. In the regime of strong Umklapp terms (to be specified later) the phase diagram is completely covered by periodic configurations, and the wave number of ordering passes through a finite number of values separated by the first order transitions, i. e. the corresponding staircase is harmless.

The article is organized as follows. In Sec. II we introduce the Landau model of uniaxial ordering with two Umklapp terms and discuss its classical mechanical counterpart. The solutions of the Euler-Lagrange equation are considered in Sec. III, and the corresponding thermodynamic phase diagrams are presented in Sec. IV. Finally, in Sec. V we discuss possible implications to the phenomena observed in real materials, and compare our results with those obtained in the previous analyses of the similar models and other theories of uniaxial IC-C ordering.

II. MODEL

We start from the assumption that the quadratic contribution to the Landau expansion has minima at wave numbers $(+Q, -Q)$, where $Q_4 < Q < Q_3$, with $Q_4 = 2\pi/4$ and $Q_3 = 2\pi/3$. Here the unit length is taken equal to the lattice constant. The distances of Q from Q_3 and Q_4 are denoted by δ_3 and δ_4 respectively, with $\delta_3 + \delta_4 = \pi/6$ (Fig. 1). From now on we shall use δ_4 as an independent control parameter. Let us furthermore specify that the order parameter is complex, $\rho e^{i\phi}$. Limiting the further analysis to the temperature range well below the critical temperature for the transition from the disordered to the incommensurate phase, we also make the usual approximation of space independent amplitude ρ^5 , and keep only the phase-dependent part of the free energy density. The latter reads

$$f(\phi, x) = \frac{1}{2} \left(\frac{d\phi}{dx} \right)^2 + B \cos [3\phi + 3(\frac{\pi}{6} - \delta_4)x] + C \cos (4\phi - 4\delta_4 x). \quad (1)$$

Here we scale the free energy functional

$$F = \int dx f(\phi, x), \quad (2)$$

by $\xi_0^2 \rho^2$, where ξ_0 is the correlation length in the x -direction. The first, gradient term in Eq. (1) is the elastic contribution which favors the incommensurate sinusoidal ordering with the wave number Q . The second and third terms are the Umklapp contributions of the third and fourth order respectively. Due to the closeness of the wave number Q to both respective commensurate wave numbers, they are presumably the leading Umklapp contributions, provided both are allowed by symmetry. Their effective strengths are denoted by coefficients B and C which are proportional to the first and the second power of the amplitude ρ respectively. They are another two control parameters (beside δ_4) of the model (1). The temperature variation of ρ is expected to be the main source of the temperature dependence of B and C .

The model (1) covers a variety of possibilities which may take place in particular physical examples. Besides the competition of each Umklapp term and the elastic term present already in basic sine-Gordon models, the essential new property of the present model is an additional competition between two Umklapp terms. The relative importance of these two terms is relied on both, the ratio of the strengths B and C and the position of the wave number Q , i. e. the ratio of δ_3 and δ_4 , so that various regimes are possible. Regarding the expansion (1) it is reasonable to expect that the relative strength of two terms varies from the dominance of the third order term ($B \gg C$) at temperatures not far below the transition from the disordered phase to the comparable values of B and C at lower temperatures. However, even when $B \gg C$, the relative weakness of the fourth order Umklapp term can be compensated by a small value of δ_4 with respect to δ_3 , i. e. by its much slower space dependence. In this case it is necessary to keep both Umklapp terms in the expansion (1). Although similar arguments may be invoked in favor of retaining some other pair of commensurate wave numbers, or even more than two of them, the example (1) seems to be the most interesting one, due to the lowest possible powers of ρ present in the coefficients B and C .

The configurations which take part in the thermodynamic phase diagram of the model (1) are the solutions of the Euler-Lagrange (EL) equation,

$$\phi'' + 3B \sin [3\phi + 3(\frac{\pi}{6} - \delta_4)x] + 4C \sin (4\phi - 4\delta_4 x) = 0, \quad (3)$$

which for given values of the control parameters have the lowest value of the free energy averaged over the macroscopic length of the system, L ,

$$\langle F \rangle = \frac{1}{L} \int dx f[\phi(x), x]. \quad (4)$$

Before developing the appropriate method for the determination of such configurations, let us put few remarks on the equation (3). From the classical mechanical side it represents the nonintegrable double resonance (i. e. double sine-Gordon) model^{31,32}, with the corresponding Hamiltonian

$$H(p_\phi, \phi, x) = \frac{p_\phi^2}{2} - B \cos [3\phi + 3(\frac{\pi}{6} - \delta_4)x] - C \cos (4\phi - 4\delta_4 x), \quad (5)$$

where $p_\phi \equiv \frac{\partial f}{\partial \phi} = \phi'$. Obviously for $B = 0$ or $C = 0$ Eqs. (3) and (5) reduce to completely integrable sine-Gordon problems. For both B and C finite, one encounters the coexistence of two overlapping resonance domains. This can be easily seen with help of Poincaré cross section. We introduce the auxiliary variable

$$\psi = \phi + \left(\frac{\pi}{6} - \delta_4\right)x, \quad (6)$$

and plot the Poincaré cross section in the phase space (ψ, p_ψ) , $\psi \equiv \psi(x_0 + 3n)$, $p_\psi \equiv \psi'(x_0 + 3n)$. Here x_0 is the starting point of integration and n is an integer. The resonance domains are situated around elliptic fixed points at $(\psi = 0, p_\psi = \frac{2\pi}{3}m)$ and $(\psi = \frac{\pi}{6}, p_\psi = \frac{\pi}{4}(2m+1))$, where m is an integer. Their respective widths are $12\sqrt{B}/\pi$ if $C = 0$ and $12\sqrt{C}/\pi$ if $B = 0$. For small values of B and C (Fig. 2a) the trajectories between two resonances conserve their topological form, while chaotic trajectories exist only very close to the separatrices of both resonances. As B and/or C increase (Fig. 2b) the separatrices burst out into stochastic layers which grow and eventually merge between resonance domains. One gradually arrives at the threshold of the stochasticity (Fig. 2c), given by the Chirikov criterion³¹

$$\frac{12}{\pi}(\sqrt{B} + \sqrt{C}) \approx 1, \quad (7)$$

at which the last KAM torus is destroyed, i. e. there are no more quasiperiodic solutions between two resonances. Chaotic trajectories are now free to diffuse through all phase space between two resonances. Let us here mention two points relevant for the further discussion. First, the widths of the chaotic layers grow exponentially³⁵ as parameters B and C increase. Thus, the area between two resonances will be rapidly covered with chaotic layers. Second, KAM tori represent the main obstacles to diffusion of chaotic trajectories through phase space (³³ and references therein).

III. SOLUTIONS OF THE EULER-LAGRANGE EQUATION

Beside the classical mechanical context, our problem has an additional aspect, namely we are looking for the thermodynamically stable solutions, i. e. the trajectories in the phase space from Figs. 2a,b,c which are local minima of the functional (2). Since we have to compare average free energies (4) of the trajectories present in the phase space, our first task is to specify numerical methods appropriate for the calculation of particular types of solutions.

The orbitally unstable periodic solutions obviously cannot be determined by a direct integration of EL equations (3), commonly used for calculation of orbitally stable solutions. It is therefore necessary to calculate them by using a suitable boundary value method for nonlinear equations. The most natural choice is the finite difference method, which is however rather demanding regarding the computer memory and time. It is therefore important to reduce the search for periodic solutions by establishing in an analytic way sufficient conditions on the possible values of periods. To this end we start from the relation

$$\phi(x + P) = \phi(x) + \phi_P, \quad (8)$$

which holds for any periodic solution. Here P is its period and ϕ_P is the phase increment per period (note that the periodic solutions with finite ϕ_P belong to the rotational part of the phase space). Inserting Eq. (8) into the EL equation (3) taken at $x + P$ one gets

$$\phi'' + 3B \sin [3\phi + 3(\frac{\pi}{6} - \delta_4)x + 3\phi_P + 3(\frac{\pi}{6} - \delta_4)P] + 4C \sin (4\phi - 4\delta_4x + 4\phi_P - 4\delta_4P) = 0, \quad (9)$$

where $\phi \equiv \phi(x)$. Sufficient conditions on the values of parameters P and ϕ_P follow from the requirement that Eqs. (9) and (3) have the same form, i. e. that

$$3\phi_P + 3(\frac{\pi}{6} - \delta_4)P = 2\pi k, \quad 4\phi_P - 4\delta_4P = -2\pi l, \quad (10)$$

where k and l are integers. Thus we get

$$P = 4k + 3l, \quad \phi_P = \delta_4P - l\frac{\pi}{2}. \quad (11)$$

Obviously, each periodic solution satisfying the requirement (10) is uniquely defined by a pair of integers (k, l) which do not have a common integer factor²⁸. Note that the above procedure, in particular the step from Eq. (9) to the conditions (10), in principle does not forbid the existence of periodic solutions which do not belong to the set defined by Eqs. (11). However, our attempts to locate numerically such solutions, although based on two independent algorithms, present and the alternative one³⁶, always led to a negative result. This is an indication that the solutions with the periods (11) are very probably the only possible periodic solutions, i. e. that the relations (10) are also the necessary conditions for their existence.

The solution $\phi(x)$ with the period (11) has the total wave number (that measured from the origin of Brillouin zone)

$$\tilde{q} \equiv Q - \frac{\phi_P}{P} \equiv 2\pi q = 2\pi \frac{k+l}{4k+3l}. \quad (12)$$

The values of q allowed by conditions (10) form a Farey tree, shown in Fig. 3 for the wave numbers between $q = 1/3$ ($k = 0, l = 1$ and $P = 3$) and $q = 1/4$ ($k = 1, l = 0$ and $P = 4$). Thus, already at this introductory stage of the analysis we conclude that the model (1) has the phase diagram with branchings between neighboring commensurate configurations equivalent to those of ANNNI models^{16,18}.

The periodic solutions $q = 1/3$ ($k = 0, l = 1$ and $P = 3$) and $q = 1/4$ ($k = 1, l = 0$ and $P = 4$) in the Farey tree of Fig. 3 are the basic commensurate configurations, belonging to the Umklapp terms of third and fourth order respectively. The wave numbers at lower levels of the Farey tree from Fig. 3 represent higher order commensurate solutions which correspond to all positive values of k and l . They are situated between two main resonances in the Poincaré cross section shown in Fig. 2. Note that for small values of B and C their positions in the phase space (Fig. 2a) perfectly match positions in the Farey tree (Fig. 3). As the parameters B and C further increase, the positions of periodic solutions that are embedded in chaotic layers become slightly intermixed since there are no more KAM tori between two resonances that restrict their positions in phase space (Fig. 2c). We do not include the parts of the Farey tree belonging to negative values of k and/or l since, as it will become clear later, they are not thermodynamically stable for $0 < \delta_4 < \pi/6$ and $B, C > 0$.

In the next step we specify boundary conditions for a particular periodic solution $\phi_{kl}(x)$. Since every periodic solution possesses at least two inflection points, we chose one of them, x_0 , to be the initial point of integration, i. e. the left end point of one period. Thus $\phi''_{kl}(x = x_0) = 0$. The boundary conditions now read

$$\begin{aligned} \phi_{kl}(x = x_0 + P) &= \phi_{kl}(x = x_0) + \phi_P, \\ \phi'_{kl}(x = x_0 + P) &= \phi'_{kl}(x = x_0). \end{aligned} \quad (13)$$

Since the values of P and ϕ_P follow from the choice of integers (k, l) (Eqs. (11)), it remains to establish the connection between the other three parameters, x_0 , $\phi_{kl}(x = x_0)$ and $\phi'_{kl}(x = x_0)$, which figure in the conditions (13). As it follows from the EL equation (3) with $x = x_0$,

$$3B \sin [3\phi(x_0) + 3(\frac{\pi}{6} - \delta_4)x_0] + 4C \sin (4\phi(x_0) - 4\delta_4 x_0) = 0, \quad (14)$$

x_0 and $\phi(x_0)$ are not independent. Even more, the numerical experience suggests that for a given periodic solution both x_0 and $\phi(x_0)$ do not vary as we change B and/or C , i. e. that Eq. (14) in fact decomposes into two conditions,

$$\begin{aligned} 3\phi(x_0) + 3(\frac{\pi}{6} - \delta_4)x_0 &= M\pi, \\ 4\phi(x_0) - 4\delta_4 x_0 &= -N\pi, \end{aligned} \quad (15)$$

where M and N are integers. This means that x_0 and $\phi(x_0)$ may have values

$$x_0 = \frac{1}{2}(4M + 3N) \quad (16)$$

and

$$\phi(x_0) = \delta_4 x_0 - \frac{\pi}{4}N. \quad (17)$$

These relations would allow for $2P$ values of x_0 and an infinite number of values for $\phi(x_0)$ (for a general value of δ_4). The further analysis of symmetry properties of the problem (3), as well as the numerical insight, however indicate that for any choice of periods P and ϕ_P this enumerable set is highly degenerate and reduces to only two distinct (nondegenerate) solutions. The convenient choices of x_0 and $\phi(x_0)$ characterizing these solutions for various combinations of odd and/or even values of integers k and l are listed in Tab. I.

The above analysis simplifies drastically the numerical procedure, since after specifying the parameters k, l, x_0 and $\phi(x_0)$, the determination of a given periodic solution follows from the variation of the single remaining parameter $\phi'(x_0)$. In accomplishing this procedure it appears convenient to eliminate, by transforming the variable $\phi(x)$, the explicit x -dependence from one of Umklapp terms in the EL equation (3), and to keep this dependence in the term with a weaker amplitude. Thus for B larger than C we use the variable $\psi(x)$ (Eq. (6)) instead of $\phi(x)$, so that the EL equation

$$\psi'' + 3B \sin (3\psi) + 4C \sin (4\psi - \frac{2\pi}{3}x) = 0, \quad (18)$$

and its solutions $\psi(x)$ do not depend on δ_4 . The corresponding free energy then acquires a δ_4 -dependent term in the form of Lifshitz invariant,

$$F = \int dx \left\{ \frac{1}{2} [\psi' - (\frac{\pi}{6} - \delta_4)]^2 + B \cos(3\psi) + C \cos(4\psi - \frac{2\pi}{3}x) \right\}, \quad (19)$$

which simplifies the calculation of the δ_4 -dependence of the averaged free energy for any particular periodic solution of the EL equation. As is visible in Fig. 4, the form of periodic solutions resembles to that of multisoliton solutions of simple sine-Gordon model (still, note the slight modulation of commensurate regions, i. e. between discommensurations) When C is larger than B , it is appropriate to introduce an analogous variable which makes the C -term x -independent, namely $\chi(x) = \phi(x) - \delta_4 x$. Again, the corresponding EL equation does not depend on δ_4 . The boundary conditions have to be modified correspondingly for both transformations.

Although the steps described above greatly simplify the numerical procedure, the finite difference method poses the limitations on the computer memory and time which do not allow us to calculate solutions with periods well above 100. Note in this respect that the nonlinearity of EL equation (3) or (18) forces us to use about 1000 mesh points per period in order to get solutions which are reliable enough.

Periodic solutions of EL equation (3) show several interesting properties which are important for analysis of phase diagrams. We notice that for some values (or ranges of values) of parameters B and C one of the two periodic solutions with the same values of k and l from Tab. I ceases to exist (see Fig. 5). In general the solutions with the lower value of averaged free energy are more robust to this disappearance. We do not go into a closer analysis of this effect, but only indicate that it seems to be closely connected with the destruction of KAM tori as B and C increase.

Another interesting property of periodic solutions is the splitting in averaged free energies of two solutions with the same values of (k, l) (see Fig. 5). As the parameter C gradually increases from zero, while keeping B fixed, values of the difference between these two energies increases, thus making one periodic solution more and more thermodynamically favorable with respect to the other. This splitting is larger for the solutions with smaller periods. The qualitative consequence is that such solutions participate over greater and greater parts of the phase diagram as parameters B and C increase.

For the calculation of quasiperiodic and chaotic trajectories we use standard, Adams or Runge-Kutta-Merson, methods for an initial value problem. Quasiperiodic trajectories, as a building objects of KAM tori, are orbitally stable³⁴. Chaotic orbits, although certainly orbitally unstable, are diffusive through all the corresponding chaotic layer in the phase space, so that by picking one of them we get practically the averaged free energy for all chaotic solutions in that layer. Thus, in order to calculate the averaged free energies of quasiperiodic and chaotic solutions we chose initial values by random (probability of picking periodic solution instead of quasiperiodic or chaotic ones is equal to zero), and carry out the integration as long as the accuracy is satisfying. The fact that the averaged free energy of quasiperiodic and chaotic solutions can be determined only to a limited accuracy was already pointed out by Fradkin et. al³⁴ who estimated the degree of accuracy for a given type of solution.

The estimation of the common averaged free energy of chaotic solutions within a given layer can be done as follows³⁷. The average value of Umklapp terms in the expression (19) is zero since these terms contain trigonometric functions with an argument which chaotically (randomly) varies with x . For the fourth order Umklapp term $\cos(4\psi - \frac{2\pi}{3}x)$ we have

$$\langle \cos(\frac{2\pi}{3}x) \cos(4\psi) \rangle = \langle \sin(\frac{2\pi}{3}x) \sin(4\psi) \rangle = 0, \quad (20)$$

while for the third order Umklapp term we have an average of $\cos 3\psi$ which is also zero. The averaged free energy is thus given by the integral of the gradient term $\frac{1}{2}[\psi' - (\pi/6 - \delta_4)]^2$. The latter depends on the position and the width of chaotic layer in the phase space, i. e. only on the dependence of ψ' on x along the trajectory in this layer.

In order to determine a solution with the lowest average free energy we follow solutions (periodic, quasiperiodic and chaotic) with initial conditions that belong to the line $(\psi(x_0) = 0, \psi'(x_0))$ in the phase space (ψ, ψ') (Fig. 2), and compute their average free energies. For small values of B and C , periodic and quasiperiodic solutions are regularly arranged in the phase space (Fig. 2a), with hardly distinguishable average free energies (Fig. 6a). In order to show that the solution with the lowest free energy is periodic, we follow downwards the branch of the Farey tree (Fig. 3) which starts at the point with the averaged free energy lower than those for neighboring points above and below this point. It is a numerical evidence that the average free energies increase (and tend to some finite value) as we go down through successive branch points, i. e. through the solution with larger and larger periods. Quasiperiodic solutions can be regarded as asymptotic limits of series of periodic solutions defined by successive branchings in the Farey tree, in which the period and the phase increment tend to infinity (but with a finite, irrational, value of q). The averaged free energies of quasiperiodic solutions thus should be equal to the limiting values of averaged free energies at a given branch, which are, as is argued above, higher than the averaged free energy of the starting periodic solution. Since

this argument is based on numerical calculations, it cannot be extended to very small values of B and C for which the solution with the lowest free energy, as well as the solutions at the accompanying branch in the Farey tree, have too large periods.

In the range of intermediate values of B and C (Fig. 6b) there are intervals of initial conditions in which quasiperiodic solutions disappear, and only chaotic and periodic solutions are present. The chaotic layers can be easily recognized in the Poincaré cross section (Fig. 2b). The average free energies of periodic solutions then look as needle-like minima immersed in the average free energy of chaotic layers, represented by plateaux in Fig. 6b. Finally, for large values of B and C (Fig. 6c) for which the Chirikov criterion (7) is fulfilled, there remains a single chaotic layer between two resonance domains (Fig. 2c), while the number of existing periodic solutions gradually decreases as B and C increase. Since there remains a finite number of corresponding well defined needle-like minima, it is sufficient to limit the numerical calculations to the search for existing periodic solutions, and to find out among them the solution that has the lowest average free energy.

IV. PHASE DIAGRAM

We have argued in the previous section that the configurations with minimal average free energy are among periodic solutions of EL equation (3). Before presenting results of numerical calculations which confirm this expectation, we briefly discuss the parameters present in the model (1).

The parameters B and C depend on external conditions, most usually on temperature and pressure. As it was mentioned in Sec. II, they depend on the amplitude of the order parameter linearly and quadratically respectively. At temperatures closely below T_I , the temperature of phase transition from the disordered to the incommensurate phase, the ratio B/C is proportional to $(T_I - T)^{-1/2}$. A more complete insight into the temperature dependence of the order parameter, and of the ratio B/C as well, in the wider temperature range below T_I , can be obtained from the neutron scattering, NMR and similar experimental data for particular materials (e. g. references^{38,39}). As for the pressure dependence of B and C , it can be specified only after the insight into the microscopic model for a particular material on which the Landau theory is based. The parameter δ_4 also might be temperature and/or pressure dependent. Usually, in a concrete physical situation certain dependences may be regarded as dominant. E. g., when temperature varies and pressure is constant δ_4 can be often regarded as constant, while B and C are temperature dependent. Having this in mind we simplify the further discussion by keeping one of the parameters fixed and concentrating on phase diagrams in remaining two-dimensional parameter subspaces.

The role of the parameter δ_4 , the position of the instability with respect to the wave number of the fourth order commensurability, is expressed through the Lifshitz invariant $\delta_4\psi'(x)$ in Eq. (19) which favors the incommensurate ordering. On the other side two Umklapp terms favor commensurate orderings with their respective wave numbers. For $\delta_4 \rightarrow 0$, and fixed values of parameters B and C , the Umklapp term of the fourth order dominates with respect to that of the third order, and the thermodynamically stable periodic solution is expected to have the wave number $q_0 = 1/4$. On the same footing, for δ_4 near $\pi/6$ (i. e. for $\delta_3 \rightarrow 0$) the stabilization of the modulation with $q_0 = 1/3$ is preferred. For $0 < \delta_4 < \pi/6$ we expect that some other higher-order wave numbers of modulation become thermodynamically stable and that they follow the order specified by the Farey tree from Fig. 3.

Let us now fix the parameter B and allow for the variation of the parameters δ_4 and C . For a particular value of C we find periodic solutions of the EL equation (18) by following the steps from Sec. III, and calculate their average free energy (19) for a relevant range of values of the parameter δ_4 . Then we determine a solution which is the absolute minimum of the average free energy for a given value of δ_4 , and in particular the isolated values of δ_4 at which first order phase transitions take place since two (or more) configurations are simultaneously absolute minima of the free energy. Varying also systematically the parameter C we obtain the phase diagram, as shown in Fig. 7 for $B = 0.02$. All lines in this diagram represent the phase transitions of the first order between the periodic configurations with different wave numbers (which are denoted only for few dominant phases in the diagram). Note that the Chirikov line (7) is at $C \approx 0.0145$, and that below $C \approx 0.01$ there is a proliferation of configurations with commensurabilities of higher and higher orders. The absence of these configurations at larger values of C is mostly due to the fact that, although they exist as solutions of the EL equation, their average free energies are too high in comparison to those of the solutions with lower commensurabilities. In addition, some periodic solutions simply cease to exist as C (or B) increase, as shown in Fig. 5. Note also that only one of two different classes of periodic solutions with the same values of k and l participates in the phase diagram in Fig. 7, i. e. that characterized by the initial conditions from the second rows (depending on evenness and oddness of integers k and l) in Tab. I. Still, we find out numerically that the average free energies for two different solutions with the same (k, l) may change order, i. e. that the solutions from the first rows in Tab. I may have lower average free energy than those from the second rows provided they are of rather high commensurability. Thus, it is somewhat surprising that in the phase diagram in Fig. 7 the periodic

solutions with only one type of boundary conditions prevail. We shall come back to this point later in Sec. V.

In addition to the phase diagram, we plot in Fig. 8 the corresponding staircase, i. e. the wave number of the stable configuration *vs* parameters C and δ_4 . As long as C is not very small there is a finite number of steps, i. e. we obtain the so-called harmless staircase, introduced by Villain and Gordon¹³. We stress that the most interesting property of the phase diagram from Figs. 7 and 8, the presence of a finite (small) number of stable commensurate configurations, is encountered in the regime of rather high values of parameters B and C . The phase portrait of the EL equation (3) is then almost everywhere chaotic (Fig. 2c) and there are no more quasiperiodic solutions between two resonances. By increasing further the values of parameters B and C one eventually comes to the phase diagram in which only two main commensurate phases ($q = 1/3$ and $q = 1/4$) take place.

Another possible presentation of the phase diagram is that with a fixed value of the parameter δ_4 and with varying parameters B and C . It is presumably closer to usual physical situations in which only weak temperature and pressure dependences of δ_4 are expected. The construction of the (B, C) phase diagram is however computationally more demanding, since one has to look for the solution with the lowest average free energy within a set of solutions for given values of B and C , i. e. one has to calculate the whole set of periodic solutions of the EL equation [Eq. (3) or (18)] for each point in the two-dimensional phase diagram. To this end we use a mesh of points which is dense enough in the (B, C) plane, and determine the solution with the lowest average free energy at each point. The phase diagram obtained in this way for $\delta_4 = \pi/12$ is shown in Fig. 9. Note that again only configurations with rather low orders of commensurability, i. e. with small values of parameters (k, l) , are present above the Chirikov line (Eq. (7)), while below this line the diagram is more complex since a great number of first order transitions takes place within a small part of the phase diagram.

V. CONCLUSION

The most important conclusions of the above analysis follow from the thermodynamic phase diagram obtained in the regime of comparable strengths of two Umklapp terms included into the Landau expansion (1). At first we emphasize that only one type of solutions of the corresponding EL equation, namely periodic configurations, participates in the phase diagram. Furthermore, all phase transitions between successive commensurate phases are of the first order, so that the wave number of ordering follows a harmless staircase with a finite number of steps. The examples of such phase diagram, namely series of successive lock-in commensurate-commensurate transitions with accompanying effects which characterize first order transitions¹⁰, are often encountered in particular materials. Here we focus our attention on few well known examples.

One of the most studied type of materials are A_2BX_4 compounds, among which we take Rb_2ZnBr_4 as a prominent representative. Early neutron diffraction measurements⁴⁰⁻⁴² of the temperature variation of modulation wave number revealed the existence of several higher-order commensurate phases. The more complete pressure-temperature phase diagram followed from various subsequent data, in particular again from the neutron diffraction measurements of Parlinski et al.^{43,44}. It resembles to a great extent to our phase diagrams from Figs. 7 and 9. Note also that the phenomenological formula for wave numbers of observed commensurate phases introduced by Parlinski et al.⁴³ coincides to our expression for Farey tree (12), which is, as is shown in Sec. III, inherent to the model (1). Harmless staircase are clearly seen in e. g. pressure variation of the wave vector for a fixed temperature⁴³, with steps going as $1/3, 7/24, 2/7$ and $1/4$ by increasing pressure. They are accompanied by hysteresis in pressure and temperature runs, which are particularly strong when only a few steps appear in the phase diagram. This corresponds to the regime of rather high values of parameters B and C , in which the phase diagram contains only few commensurate phases and the average free energy of chaotic plateau is well above average free energies of periodic solutions (Fig. 6c).

Existing theoretical approaches to the (in)commensurate orderings in A_2BX_4 compounds, in particular to the appearance of series of commensurate phases, are mostly phenomenological, based either on Landau expansions⁴⁵ or on the discrete models of competing local interactions^{17,20,21}. The justification for the continuous Landau models, which are generally appropriate to weak coupling systems, comes from many experimental indications, starting from the early neutron scattering data⁴⁰⁻⁴², showing a well-defined dispersion curves for collective modes with distinct soft-mode minima. However, the previous analyses of Landau models were restricted to purely sinusoidal modulation, and, as such were not able to explain the appearance of phases with commensurabilities of orders higher than three or four. It was therefore proposed that such phases appear due to the presence of Umklapp terms of higher orders in the free energy expansion²²⁻²⁴. This explanation, which is based on the assumption that distinct commensurate stars of wave vectors are necessary for the stabilization of, presumably sinusoidal, phases with corresponding wave vectors²²⁻²⁴, is not convincing since the Umklapp terms of order higher than four are expected to be negligible in weakly coupled systems with a displacive order.

For these reasons the more recent attempts turned again towards another type of approaches, those which assume

strong couplings, so that the lattice discreteness has to be taken into account. Originally the sequences of IC-C and C-C phase transitions were within this scheme interpreted in terms of the FK model as devil's staircase dependences of the wave number of ordering, i. e. as dense sequences of second order phase transitions³. However, observed staircase rarely resemble, even within experimental limitations, to the dense devil's staircase. Beside, phase transitions between successive C phases are usually of the first order. The phase diagrams which are closer to experimental findings may be however obtained by various extensions of the basic FK model, e. g. by including an additional harmonic potential^{46,47}. Also, the more complex models of competing interactions, e. g. DIFFOUR¹⁴ and ANNNI¹⁵⁻¹⁸ models, as well as models that assume two critical modes per lattice site^{20,21}, are particularly successful in describing the phase transitions in A_2BX_4 compounds. Within some of these models (e. g. Refs.²⁰ and²¹) one also obtains the first order phase transitions between configurations having the same wave numbers but different symmetries. As was already stated in Sec. IV, this is not the case within the model (1), i. e. although the EL equation (3) may possess two types of solutions with the same periods, only one type of solutions participates in the phase diagram.

The present analysis again starts from the minimal Landau expansion (with terms up to the fourth order), but takes into consideration all solutions of the corresponding EL equation. In particular it indicates that the theoretical approach⁴⁰, proposed together with the first neutron scattering measurements on Rb_2ZnBr_4 , might be essentially sufficient for the understanding of complex phase diagrams in A_2BX_4 materials. The more detailed analysis which takes into account some additional aspects, like the couplings to the homogeneous polarization and strain which appear in some materials as secondary order parameters, will be done elsewhere.

Betaine-calciumchloride-dihydrate (BCCD), together with its deuterated version D-BCCD, belongs to the second type of intensely studied materials with the commensurate lock-ins. It shows an exceptionally rich staircase going from $q = 1/3$ down to $q = 0$, with numerous intermediate steps of higher orders⁴⁸⁻⁵⁰. A closer insight into the region of phase diagram with the wave number between $q = 1/3$ and $q = 1/4$ shows that only upper right triangle of the Farey tree from Fig. 3 is realized, i. e. the phase diagram is mostly covered by wave vectors close to $q = 1/4$, and not by those close to $q = 1/3$. This sequence of IC-C transitions was successfully interpreted within various discrete models with competing interactions, e. g. in Refs.^{51,52}. Within the model (1) such phase diagram corresponds to the regime in which the fourth order Umklapp term dominates with respect to that of the third order. Also, two types of extensions of our model may lead to the stabilization of commensurate phases with $q < 1/4$. Namely, one may allow for negative values of the parameter δ_4 , or start with other Umklapp terms, e. g. with those of the fourth and fifth order, and pursue the analysis analogous to that of Secs. III and IV.

We also mention some other materials that exhibit a sequence of IC-C and C-C phase transitions between $q = 1/3$ and $q = 1/4$, but are not so extensively studied as previous two examples. E. g., Dénoyer et al.⁵³ investigated NH_4HSeO_4 and its deuterated version ND_4DSeO_4 by neutron diffraction, and found the harmless staircase and first order phase transitions, accompanied by the coexistence of several phases in the relatively wide range of temperatures. A series of IC-C and C-C phase transitions are also observed in $BaZnGeO_4$ in X-ray diffraction measurements by Sakashita et al.⁵⁴, and in electron diffraction measurements by Yamamoto et al.⁵⁵ which also provide dark field images of discommensurations appearing in the vicinity of $q = 1/3$ phase. An example of particularly sharp transition from $q = 1/3$ to $q = 1/4$, with a very wide temperature range of the coexistence of these two commensurate phases, was found by Broda⁵⁶ in $(NH_4)_2CoCl_4$, the material that also belongs to A_2BX_4 family.

The free energy (1) is similar to that of Fradkin et al.³⁴ who also studied continuum systems with competing periodicities. The only difference between two expressions is the absence of the factors 3 and 4 in front of the variable $\phi(x)$ in the cosine terms of the model³⁴. However, in contrast to ours, the analysis carried out in Ref.³⁴ is limited to the close vicinity of the separatrices (and hyperbolic points) in the phase space³¹, i. e. to the dilute soliton lattices. Then the continuum model can be converted into a discrete mapping of the FK type, analyzed in detail previously by Aubry³. Our analysis covers the whole phase space, i. e. all solutions of the EL equation (3), and in particular the whole class of periodic configurations. In particular, our thermodynamic phase diagram (Figs. 7 and 9) includes, in contrast to that of Ref.³⁴, the most interesting part of the phase space, namely that between two resonances (i. e. sets of hyperbolic points).

The model³⁴ was the starting point in the investigation⁵⁷ of the memory effects in systems with IC modulations, based on the earlier proposition⁵⁸ that mobile defects might be responsible, by forming defect density waves, for the sensitivity of the IC ordering on the thermal history of crystal, observed e. g. in thiourea⁵⁹. Errandonea⁵⁷ argued that the double sine-Gordon model, with two lock-in potentials originating from the lattice the defect density wave, is an appropriate description of this phenomena.

The model (1) provides the explanation of memory effects (together with thermal hystereses), without referring, in contrast to models^{57,58}, to defects as an intrinsic ingredient of the theory. At first, we note that the crossings of lines of first order phase transitions in Figs. 7, 8 and 9 are accompanied by hystereses. Our preliminary analysis³⁶ indicates that these hystereses may be rather wide on e. g. temperature scale. Furthermore, the present analysis of the EL equation (3) shows that periodic solutions, which constitute the phase diagram, are immersed as isolated points into the environment of chaotic configurations. This environment prevents both, the continuous variation of

the wave number of ordering and the continuous phase transitions of the second and higher orders. The average free energy of chaotic solutions from Fig. 6c is the measure of the energetic barrier which the system has to overcome in order to pass from some periodic (metastable) configuration to another one with lower free energy. This is expected to be a common property of models which are nonintegrable (beside being nonlinear), and have thermodynamically stable periodic configurations isolated in the chaotic phase space¹².

The memory effects are also observed in class II of IC systems¹⁰. The detailed analysis of phase diagram for this class³⁰ led to the conclusion that the corresponding phenomena seen in particular materials may be as well interpreted in terms similar to those presented above. However, it was also stressed³⁰ that defects may have a secondary role as triggers which favor the stabilization of some domain patterns. This interpretation invokes neither the mobility of defects nor the formation of defect density waves. The analogous secondary influence of defects on memory phenomena is expected also in presently investigated systems of class I.

Finally, let us mention a common problem that arises in the analysis of continuous nonintegrable Landau models for uniaxial systems of classes I²⁸ and II³⁰, in which periodic solutions have an essential role in the extremalization of corresponding thermodynamic functionals. We remind that there is no firm universal principle which would favor the thermodynamic stability of the (meta)stable periodic configurations on account of other, quasiperiodic or chaotic, solutions of EL equations. Some hints in this direction for "autonomous" functionals (those for which the free energy density does not depend explicitly on x) follow from the recently derived general criteria⁶⁰ based on the additional extremalizations (like e. g. those involving boundary conditions). However, these criteria cannot be directly applied to the present model since the explicit x -dependence in Eq. (1) introduces fundamental singularities in the additional extremalizations⁶⁰. Thus, the most important property of the phase diagrams from Figs. 7 and 9, their complete coverage by a finite number of periodic configurations, still awaits for a deeper understanding.

We acknowledge numerous useful discussions with V. Dananić. The work is supported by the Ministry of Science and Technology of the Republic of Croatia through the project no. 119201.

- ¹ T. Janssen, in *Incommensurate Phases in Dielectrics*, edited by R. Blinc and A. P. Levanyuk (North-Holland, Amsterdam, 1986), Vol. 1, p. 67.
- ² B. Neubert, M. Pleimling and R. Siems, *Ferroelectrics* **208-209**, 141 (1998).
- ³ S. Aubry, *J. Physique* **44**, 147 (1983), and in *Statics and dynamics of nonlinear systems*, edited by G. Benedek, H. Bilz and R. Zeyher (Springer-Verlag, Berlin, 1983), p. 126.
- ⁴ P. Bak, *Rep. Prog. Phys.* **45**, 587 (1982).
- ⁵ W. L. McMillan, *Phys. Rev. B* **14**, 1496 (1976).
- ⁶ R. A. Cowley and A. D. Bruce, *J. Phys. C* **11**, 3577 (1978); A. D. Bruce, R. A. Cowley and A. F. Murray, *ibid.* **11**, 3591 (1978).
- ⁷ J. C. Tolédano and P. Tolédano, *The Landau Theory of Phase Transitions* (World Scientific, Singapore, 1987).
- ⁸ P. Bak and V. J. Emery, *Phys. Rev. Lett.* **36**, 978 (1976).
- ⁹ L. N. Bulaevskii and D. I. Khomskii, *Zh. Eksp. Teor. Fiz.* **74**, 1863 (1978) [*Sov. Phys. JETP* **74**, 971 (1978)].
- ¹⁰ H. Z. Cummins, *Phys. Rep.* **185**, 211 (1990).
- ¹¹ *Incommensurate Phases in Dielectrics*, edited by R. Blinc and A. P. Levanyuk (North-Holland, Amsterdam, 1986), Vols. 1 and 2.
- ¹² A. Bjeliš and S. Barišić, *Phys. Rev. Lett.* **48**, 684 (1982); S. Barišić and A. Bjeliš, in *Electronic properties of organic materials with quasi-one-dimensional structure*, edited by H. Kamimura (Riedel Publ. Comp., New York, Dordrecht, 1985), p. 49.
- ¹³ J. Villain and M. Gordon, *J. Phys. C* **13**, 3117 (1980).
- ¹⁴ T. Janssen and J. A. Tjon, *Phys. Rev. B* **24**, 2245 (1981); T. Janssen and J. A. Tjon, *ibid.* **25**, 3767 (1982).
- ¹⁵ M. E. Fisher and W. Selke, *Phys. Rev. Lett.* **44**, 1502 (1980).
- ¹⁶ W. Selke and P. M. Duxbury, *Z. Phys. B* **57**, 49 (1984).
- ¹⁷ Y. Yamada and N. Hamaya, *J. Phys. Soc. Jpn.* **52**, 3466 (1983).
- ¹⁸ W. Selke, M. Barreto and J. Yeomans, *J. Phys. C* **18**, L393 (1985).
- ¹⁹ W. Selke, *Phys. Rep.* **170**, 213 (1988).
- ²⁰ Z. Y. Chen and M. B. Walker, *Phys. Rev. B* **43**, 5634 (1991).
- ²¹ T. Janssen, *Ferroelectrics* **124**, 41 (1991); *Z. Phys. B* **86**, 277 (1992).
- ²² H. Mashiyama, *J. Phys. Soc. Jpn.* **49**, 2270 (1980).
- ²³ G. Marion, R. Almairac, M. Ribet, U. Steigenberger, and C. Vettier, *J. Physique* **45**, 929 (1984).
- ²⁴ K. Parlinski and F. Dénoyer, *J. Phys. C* **18**, 293 (1985).
- ²⁵ J. L. Ribeiro, J. C. Tolédano, M. R. Chaves, A. Almeida, H. E. Müser, J. Albers, A. Klöpperpieper, *Phys. Rev. B* **41**, 2343

- (1990).
- ²⁶ D. G. Sannikov, Zh. Eksp. Teor. Fiz. **96**, 2197 (1989) [Sov. Phys. JETP **69**, 1244 (1989)]; Zh. Eksp. Teor. Fiz. **97**, 2024 (1990) [Sov. Phys. JETP **70**, 1144 (1990)].
- ²⁷ D. G. Sannikov and G. Schaack, J. Phys.: Condens. Matter **10**, 1803 (1998).
- ²⁸ A. Bjeliš and M. Latković, Phys. Letters A **198**, 389 (1995).
- ²⁹ A. Michelson, Phys. Rev. B **16**, 577 (1977).
- ³⁰ V. Dananić, A. Bjeliš, M. Rogina and E. Coffou, Phys. Rev. A **46**, 3551 (1992); V. Dananić and A. Bjeliš, Phys. Rev. E **50**, 3900 (1994).
- ³¹ B. V. Chirikov, Phys. Rep. **52**, 263 (1979).
- ³² D. F. Escande and F. Doveil, Phys. Lett. A **83**, 307 (1981); J. Stat. Phys. **26**, (1981); D. F. Escande, Phys. Rep. **121**, 165 (1985).
- ³³ G. M. Zaslavsky and S. S. Abdullaev, Phys. Rev. E **51**, 3901 (1995).
- ³⁴ E. Fradkin, O. Hernandez, B. A. Huberman and R. Pandit, Nucl. Phys. B **215**, 137 (1983).
- ³⁵ R. S. MacKay, J. D. Meiss and I. C. Percival, Physica **13D**, 55 (1984).
- ³⁶ V. Dananić, M. Latković and A. Bjeliš, unpublished.
- ³⁷ V. Dananić, private communication.
- ³⁸ R. Blinc, P. Prelovšek, V. Rutar, J. Seliger and S. Žumer, in *Incommensurate Phases in Dielectrics*, edited by R. Blinc and A. P. Levanyuk (North-Holland, Amsterdam, 1986), Vol. 1, p. 143.
- ³⁹ R. Blinc, I. P. Aleksandrova, A. S. Chaves, F. Milia, V. Rutar, J. Seliger, B. Topič, S. Žumer, J. Phys. C **15**, 547 (1982).
- ⁴⁰ M. Iizumi, J. D. Axe, G. Shirane and K. Shimaoka, Phys. Rev. B **15**, 4392 (1977).
- ⁴¹ C. J. de Pater, J. D. Axe and R. Currat, Phys. Rev. B **19**, 4684 (1979).
- ⁴² M. Iizumi and K. Gesi, J. Phys. Soc. Jpn. **52**, 2526 (1983).
- ⁴³ K. Parlinski, R. Currat, C. Vettier, I. P. Aleksandrova, G. Eckold, Phys. Rev. B **46**, 106 (1992).
- ⁴⁴ K. Parlinski, R. Currat, C. Vettier, I. P. Aleksandrova, G. Eckold, Phase Transitions **43**, 183 (1993).
- ⁴⁵ Y. Ishibashi, in *Incommensurate Phases in Dielectrics*, edited by R. Blinc and A. P. Levanyuk (North-Holland, Amsterdam, 1986), Vol. 2, p. 49.
- ⁴⁶ R. B. Griffiths and W. Chou, Phys. Rev. Lett. **56**, 1929 (1986); W. Chou and R. B. Griffiths, Phys. Rev. B **34**, 6219 (1986).
- ⁴⁷ C. S. O. Yokoi, Phys. Rev. B **38**, 634 (1988).
- ⁴⁸ J. M. Kiat, G. Calvarin, M. R. Chaves, A. Almeida, A. Klöpperpieper, J. Albers, Phys. Rev. B **52**, 798 (1995).
- ⁴⁹ M. R. Chaves, J. M. Kiat, W. Schwarz, J. Schneck, A. Almeida, A. Klöpperpieper, H. E. Müser, J. Albers, Phys. Rev. B **48**, 5852 (1993).
- ⁵⁰ M. R. Chaves, A. Almeida, J. M. Kiat, J. C. Tolédano, J. Schneck, R. Glass, W. Schwarz, J. L. Ribeiro, A. Klöpperpieper, J. Albers, Phys. Stat. Sol. (b) **189**, 97 (1995).
- ⁵¹ C. Kappler and M. B. Walker, Phys. Rev. B **48**, 5902 (1993).
- ⁵² B. Neubert, M. Pleimling, T. Tentrup, and R. Siems, Ferroelectrics **155**, 359 (1994).
- ⁵³ F. Dénoyer, A. Rozycki, K. Parlinski, M. More, Phys. Rev. B **39**, 405 (1989).
- ⁵⁴ H. Sakashita, H. Terauchi, N. Tanba, Y. Ishibashi, J. Phys. Soc. Jpn. **55**, 3918 (1986).
- ⁵⁵ N. Yamamoto, M. Kikuchi, T. Atake, A. Hamano and Y. Saito, J. Phys. Soc. Jpn. **61**, 3178 (1992).
- ⁵⁶ H. Broda, Phys. Stat. Sol.(a) **82**, K117 (1984).
- ⁵⁷ G. Errandonea, Phys. Rev. B **33**, 6261 (1986).
- ⁵⁸ P. Lederer, G. Montambaux, J. P. Jamet and M. Chauvin, J. Physique Lett. **45**, L627 (1984).
- ⁵⁹ J. P. Jamet and P. Lederer, J. Physique Lett. **44**, L257 (1983).
- ⁶⁰ V. Dananić and A. Bjeliš, Phys. Rev. Lett. **80**, 10 (1998).

TABLE I. The set of possible values of x_0 and $\phi(x_0)$ needed for specifying boundary conditions of EL equation (3).

k	l	P	x_0	$\phi(x_0)$
odd	odd	odd	0	0
			0	π
even	odd	odd	0	0
			0	π
odd	even	even	0	0
			1/2	$\frac{1}{2}\delta_4 + \frac{\pi}{4}$

FIG. 1. Brillouin zone with the soft-mode minimum at Q , and the commensurate wave numbers of third (Q_3) and fourth (Q_4) order.

FIG. 2. The Poincaré cross sections for the Euler-Lagrange equation (18) and the choice of parameters: $x_0 = 1.5$, $\psi(x_0) = 0$, $B = C = 0.002$ (a), $B = 0.008$, $C = 0.006$ (b), $B = C = 0.02$ (c). The period which defines the section is equal to 3. Symbols for the periodic solutions (k, l) are: solid \circ (0,1), solid \square (1,0), solid \diamond (1,1), solid \triangle (1,2), solid \triangleleft (1,3), solid ∇ (1,4), solid \triangleright (2,1), $+$ (2,3), \times (3,1), $*$ (3,2).

FIG. 3. Farey tree for wave numbers q defined by Eq. (12).

FIG. 4. The periodic solutions $\psi(x)$ from the class $(1, l)$. The parameters are: $B = 0.02$, $C = 0.02$, $x_0 = 1.5$, $\psi(x_0) = 0$.

FIG. 5. Average free energies of the periodic solutions from the class $(1, l)$ as the function of C for $B = 0.02$ and $\delta_4 = \pi/12$. Figure (b) is the enlarged detail of the figure (a) with energies lower than 0.01. Solutions with lower average free energies are those from the second rows in Tab. I. Note from the figure (b) that e. g. the upper solution (1,6) does not exist for few subranges of the values of parameter C , and that both solutions from this class cease to exist for $C > 0.03$.

FIG. 6. Average free energy *vs* ψ'_0 of periodic (\triangle), quasiperiodic (\circ) and chaotic (solid \diamond) solutions, for $B = 0.002$, $C = 0.002$ (a), $B = 0.008$, $C = 0.006$ (b), $B = 0.02$, $C = 0.02$ (c), and $\delta_4 = \pi/12$, $x_0 = 1.5$. The (k, l) indices for the periodic solution with the lowest average free energy (solid \triangle) are (3,4) in the figures (a) and (b), and (1,1) in the figure (c). The insets in figures (a) and (b) are enlarged neighborhoods of the free energy minima.

FIG. 7. Phase diagram in the (C, δ_4) plane for $B = 0.02$. The numbers in the figure are periods of some stable commensurate phases. The dashed line at $C \approx 0.0145$ represents the Chirikov criterion (7).

FIG. 8. The wave number of modulation q_0 *vs* C and δ_4 for $B = 0.02$. The dotted cross-section represents the Chirikov criterion (7).

FIG. 9. Phase diagram in the (B, C) plane for $\delta_4 = \pi/12$. The numbers in the figure are periods of some stable commensurate phases. The dashed curve represents the Chirikov criterion (7).

Fig. 1

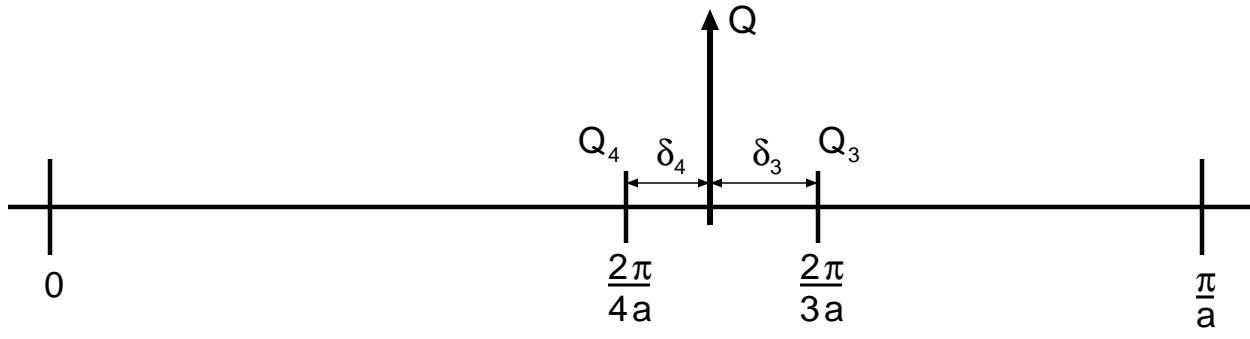


Fig. 2

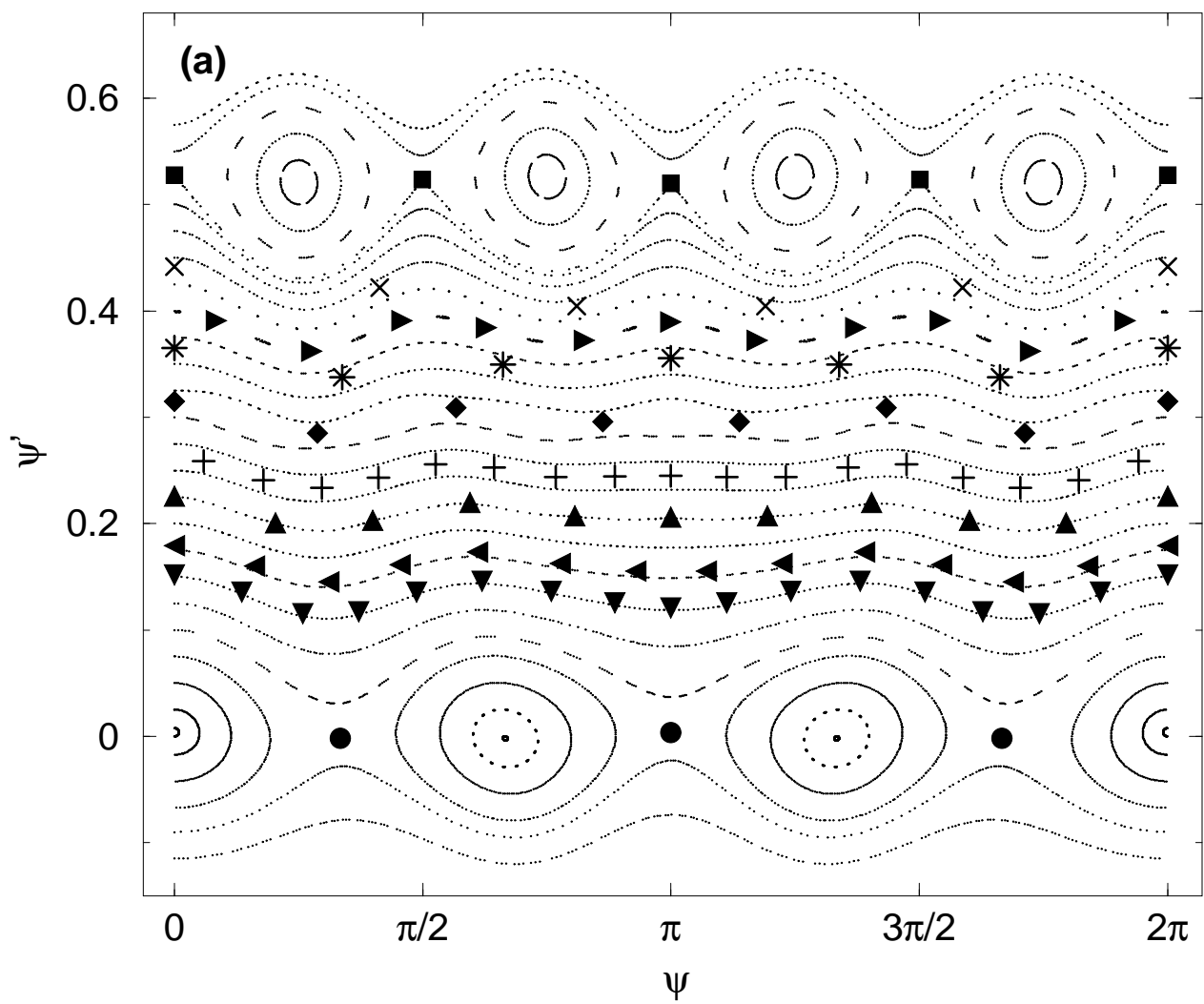


Fig. 2

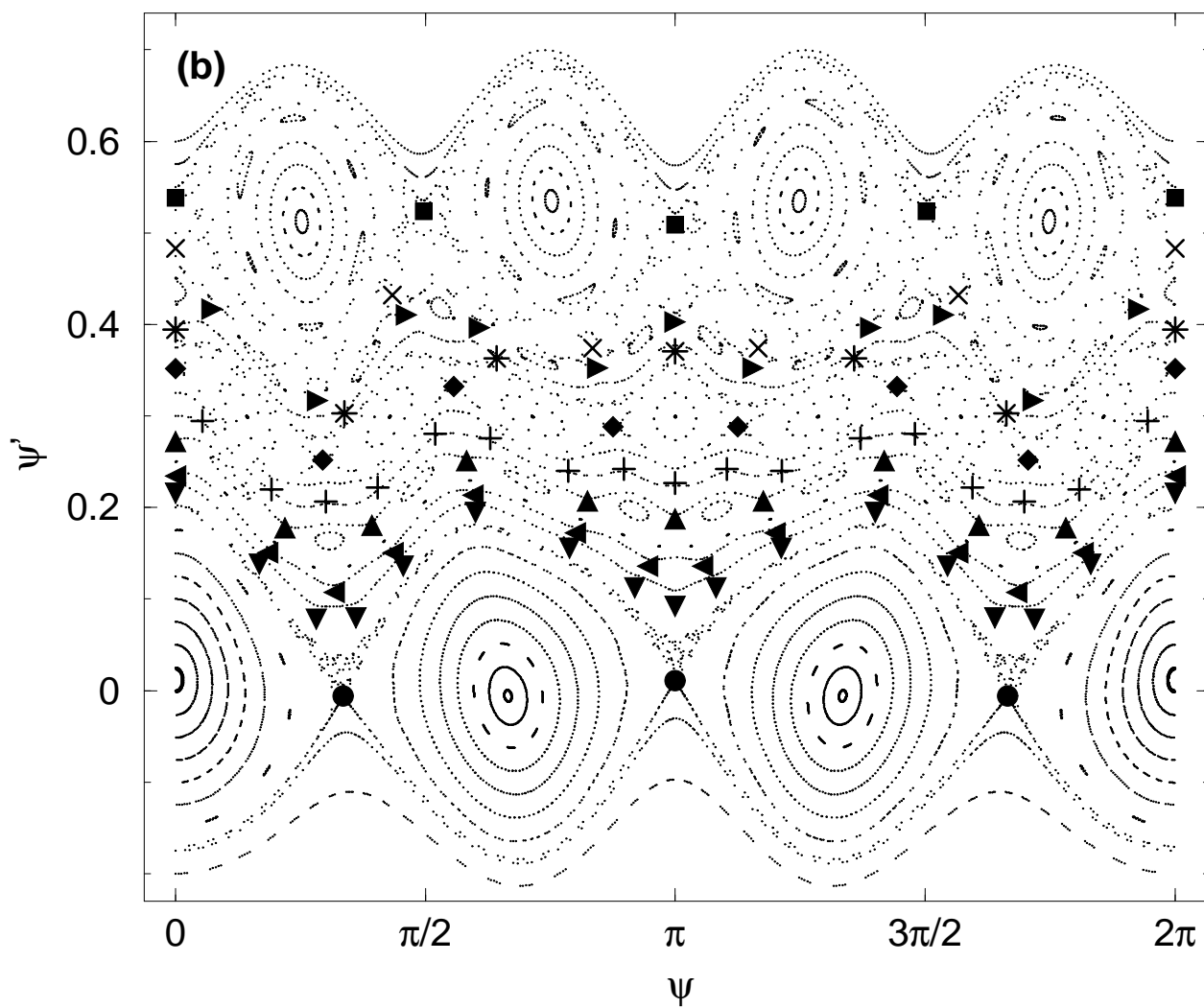


Fig. 2

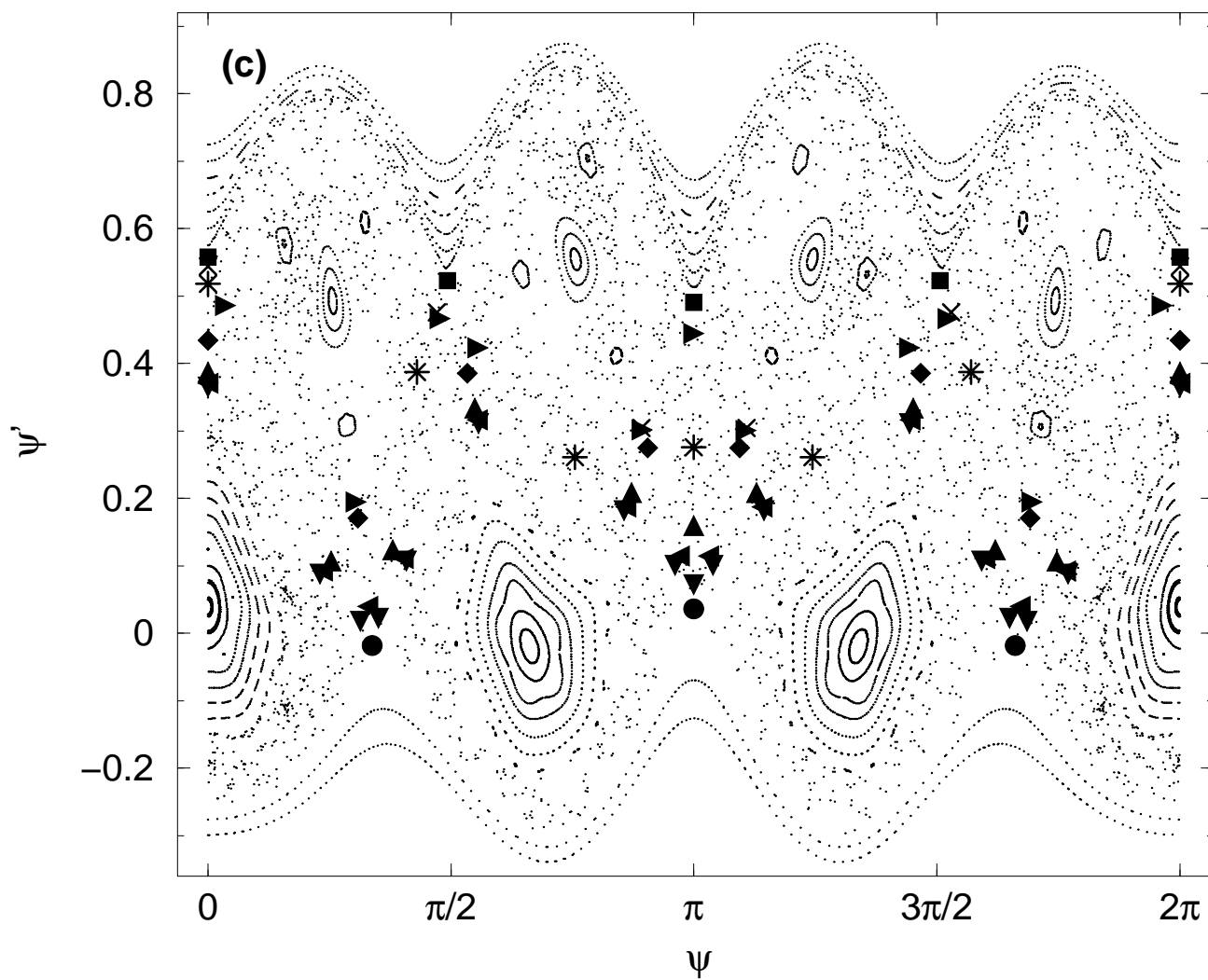


Fig. 3

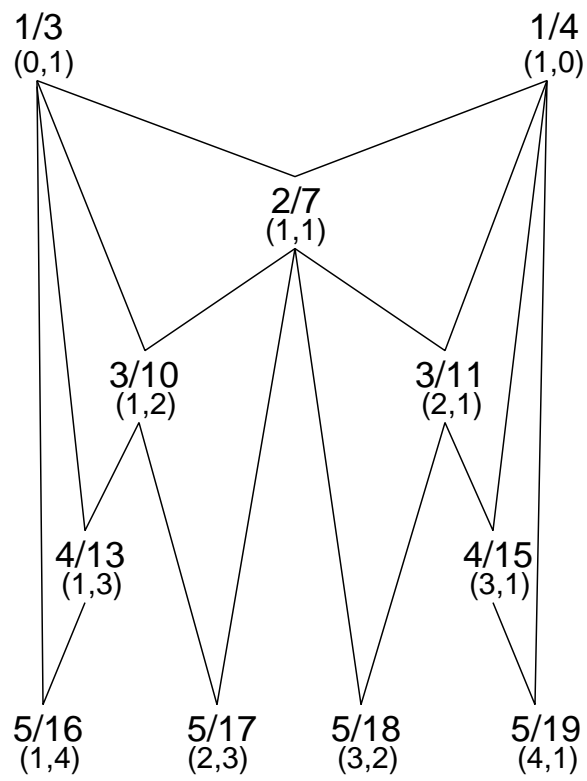


Fig. 4

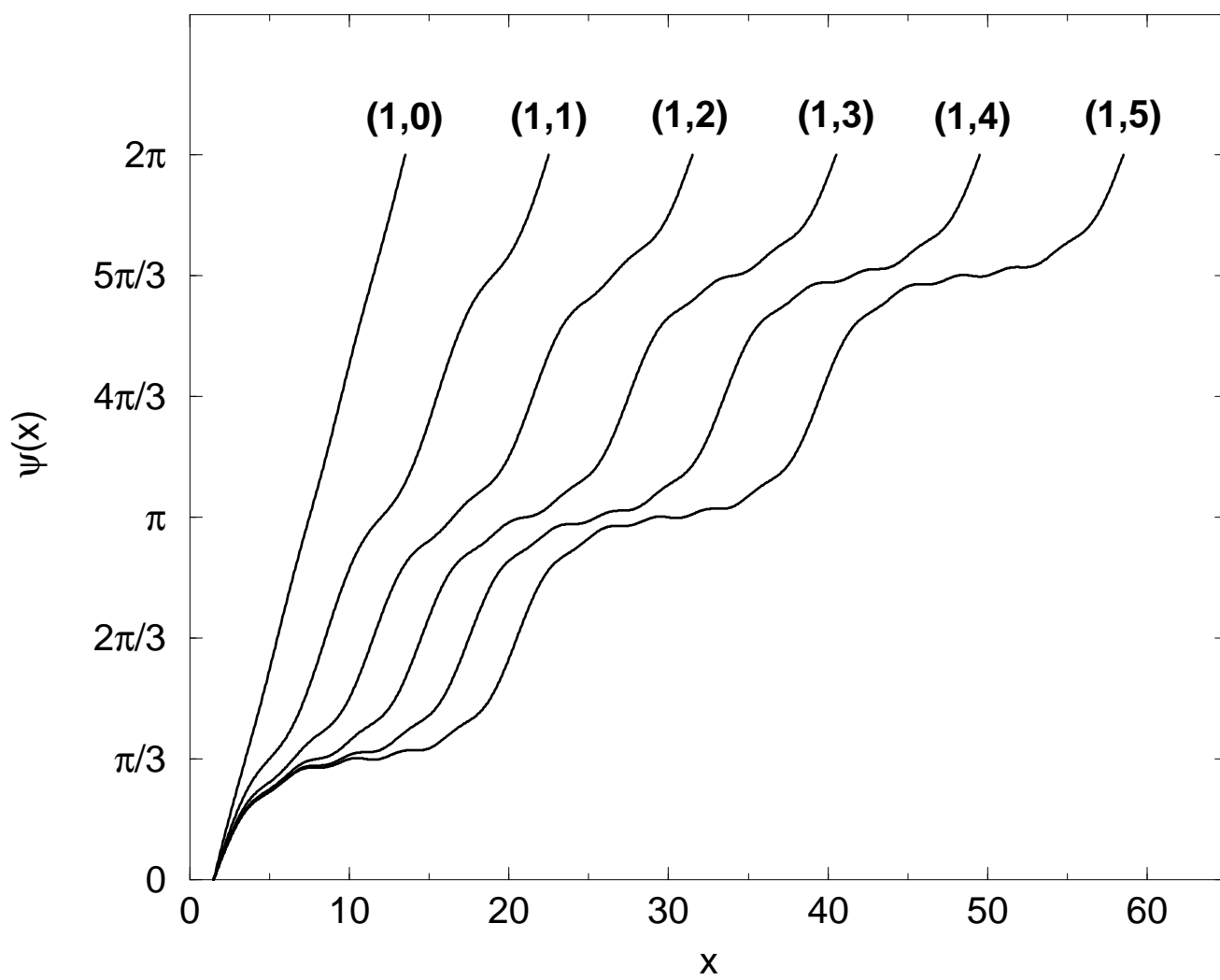


Fig. 5

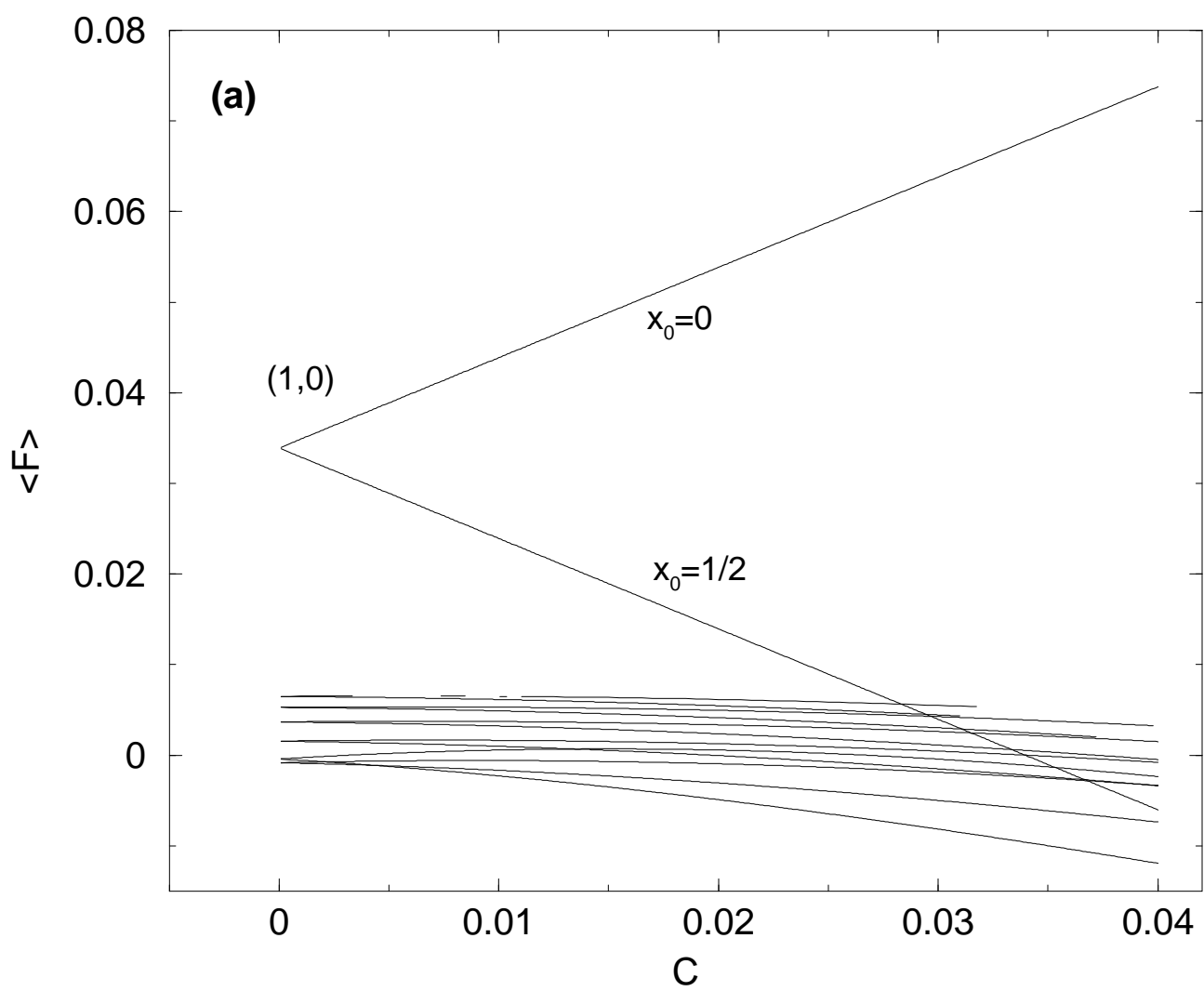


Fig. 5

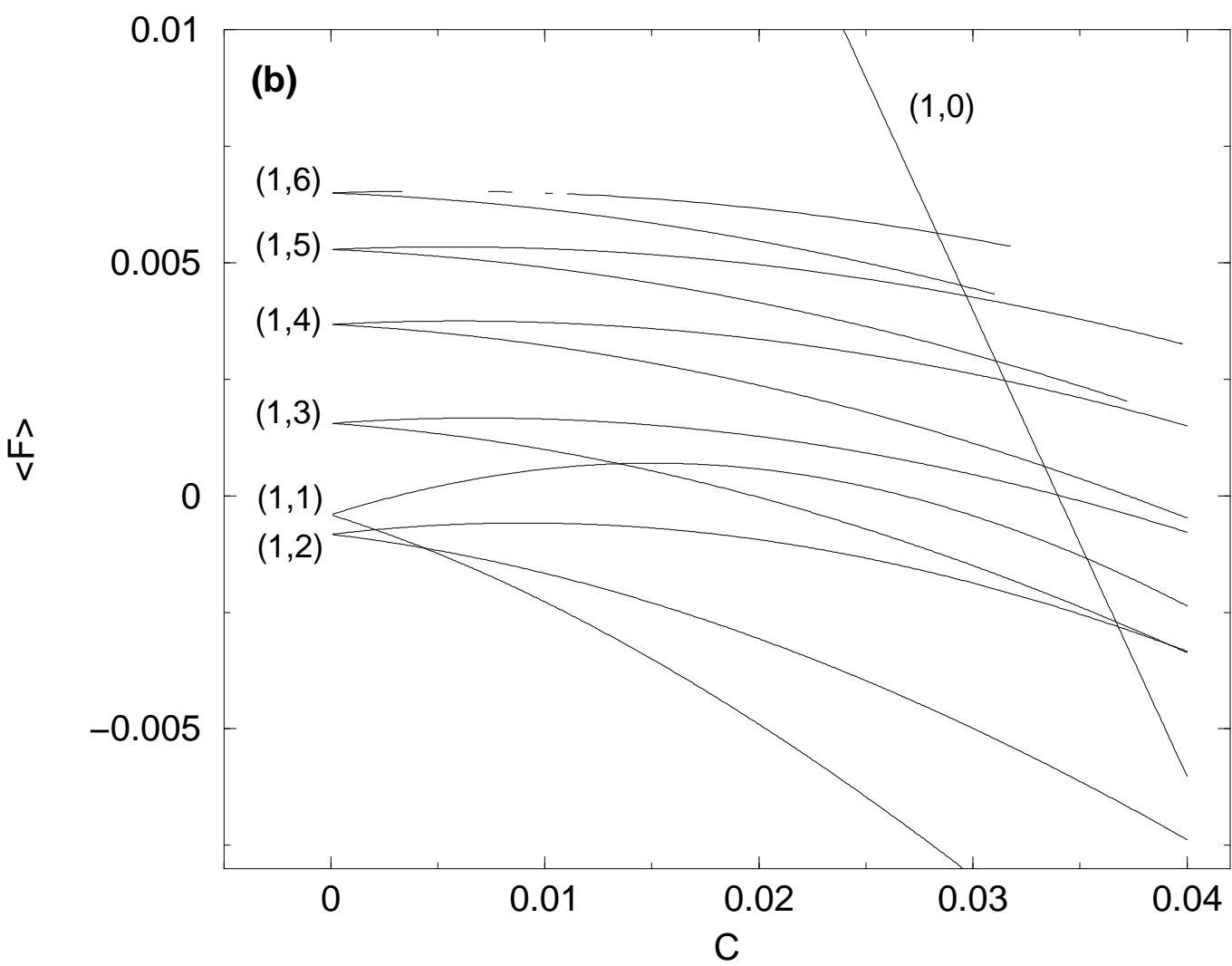


Fig. 6

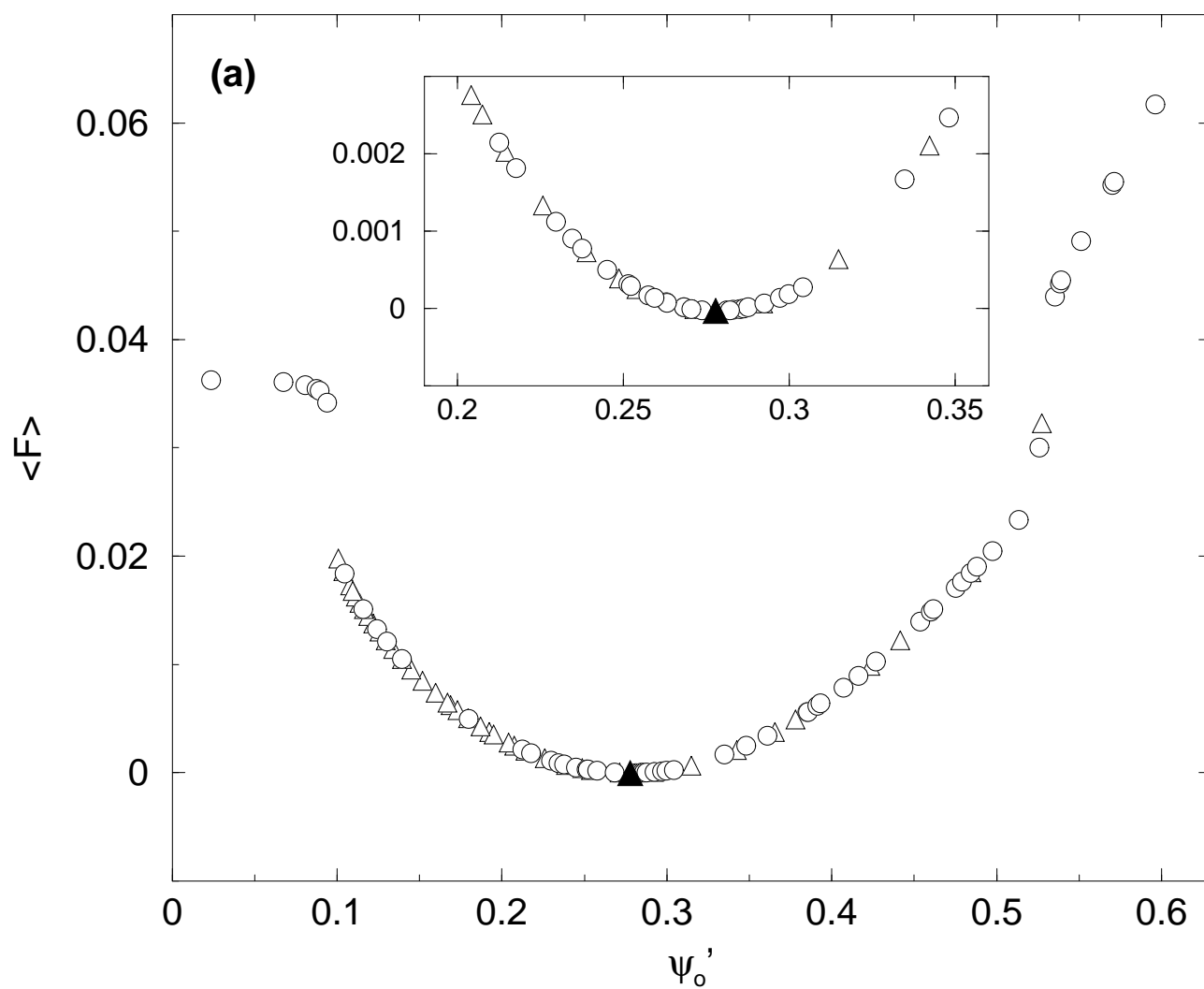


Fig. 6

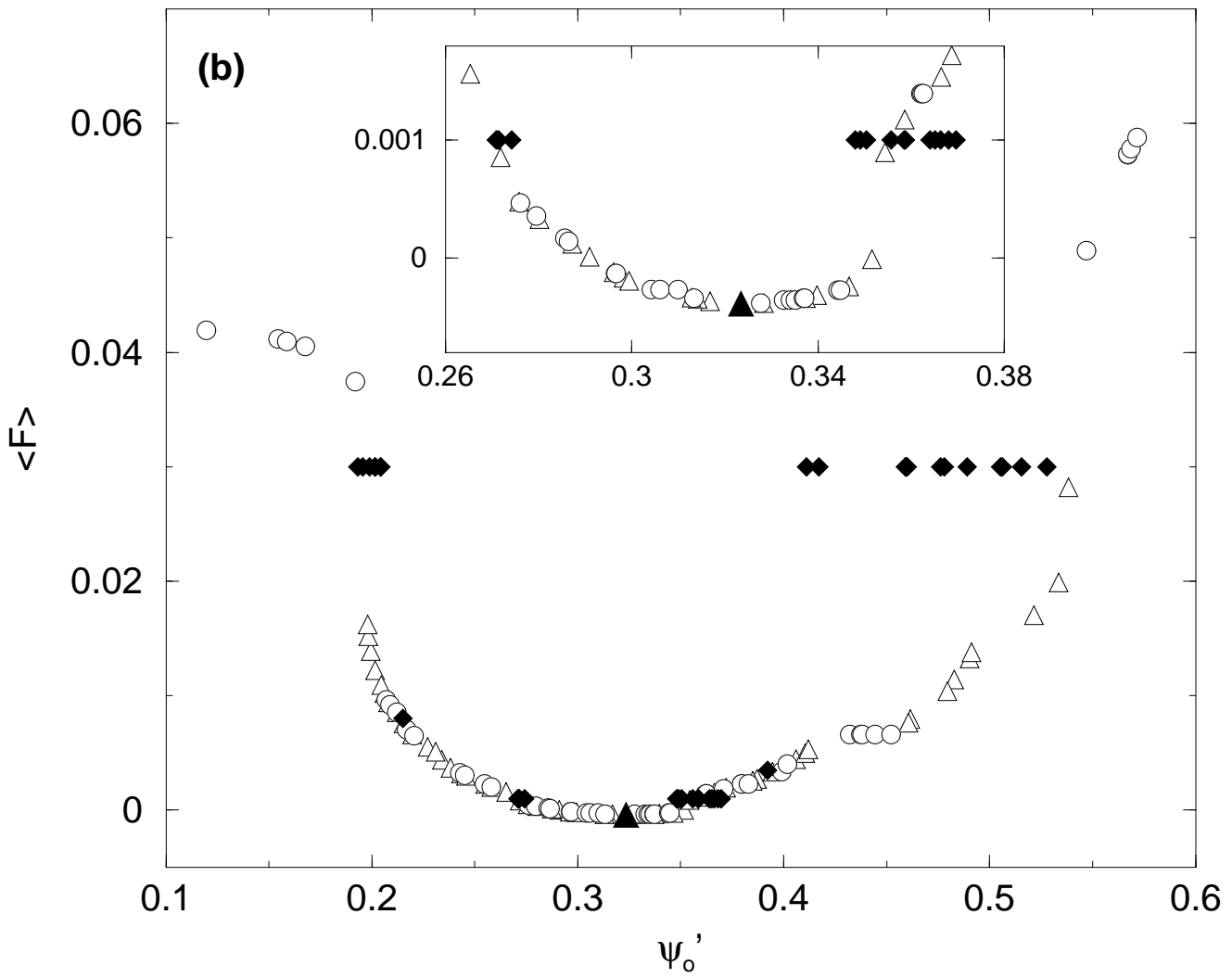


Fig. 6

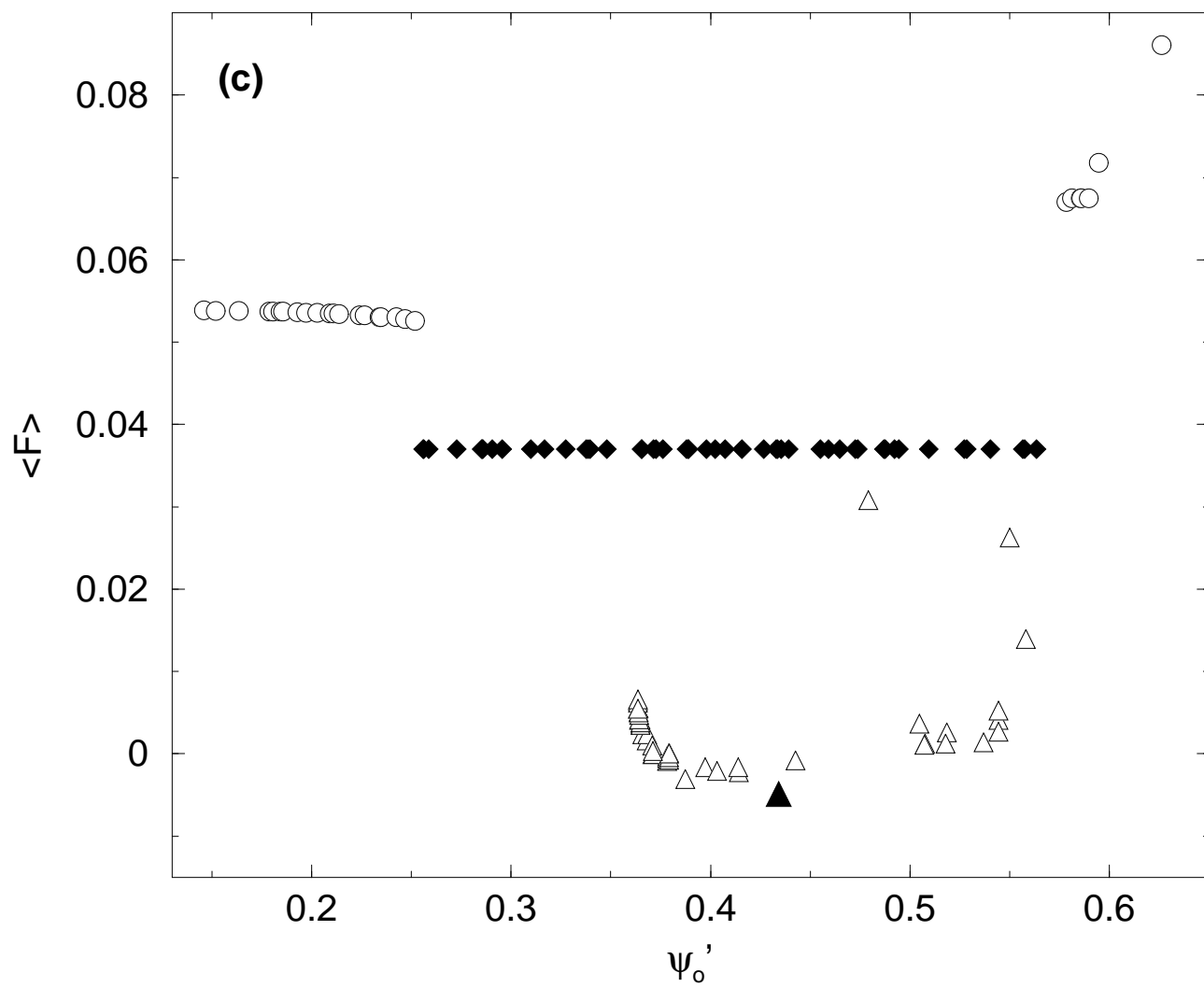


Fig. 7

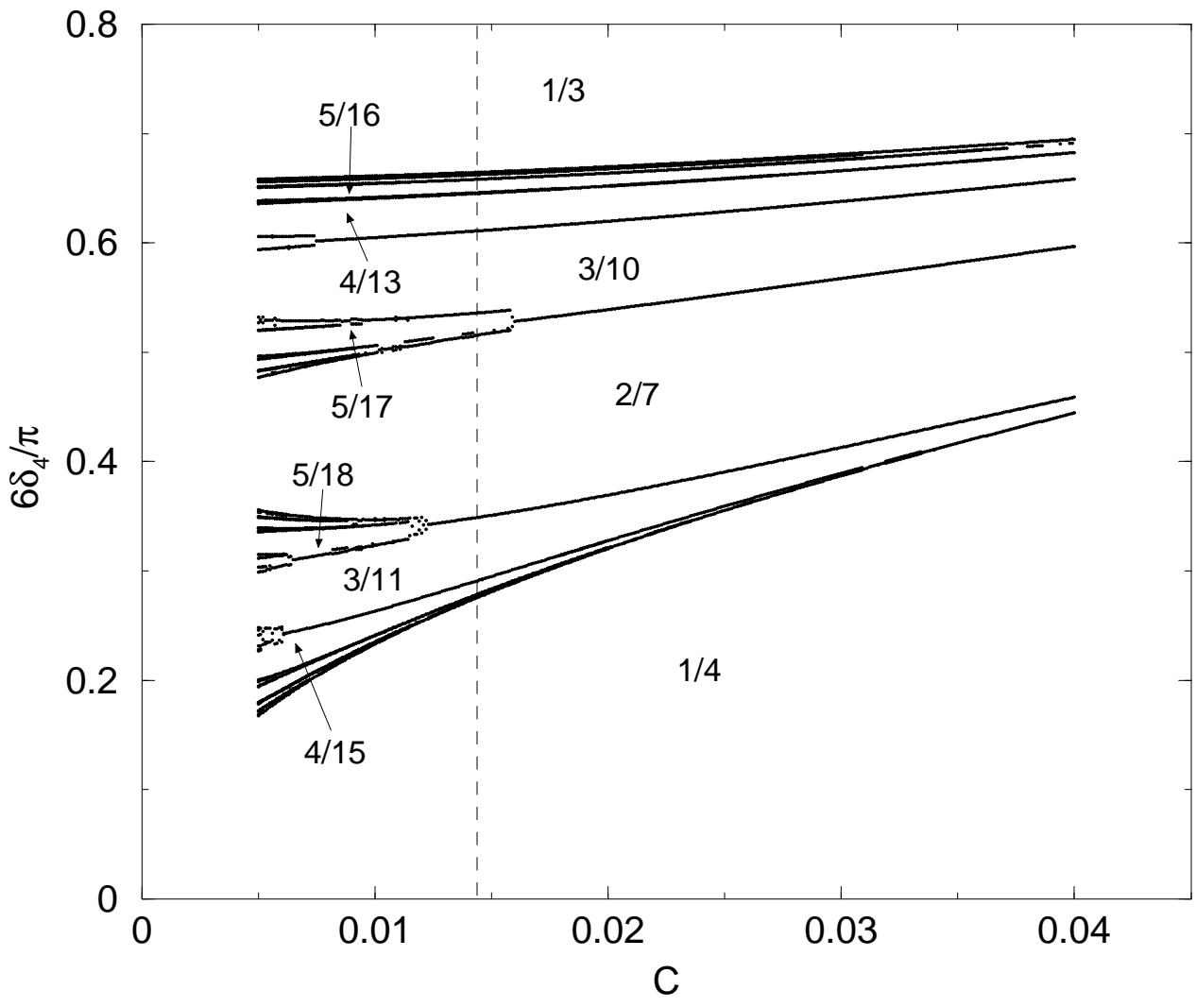


Fig. 8

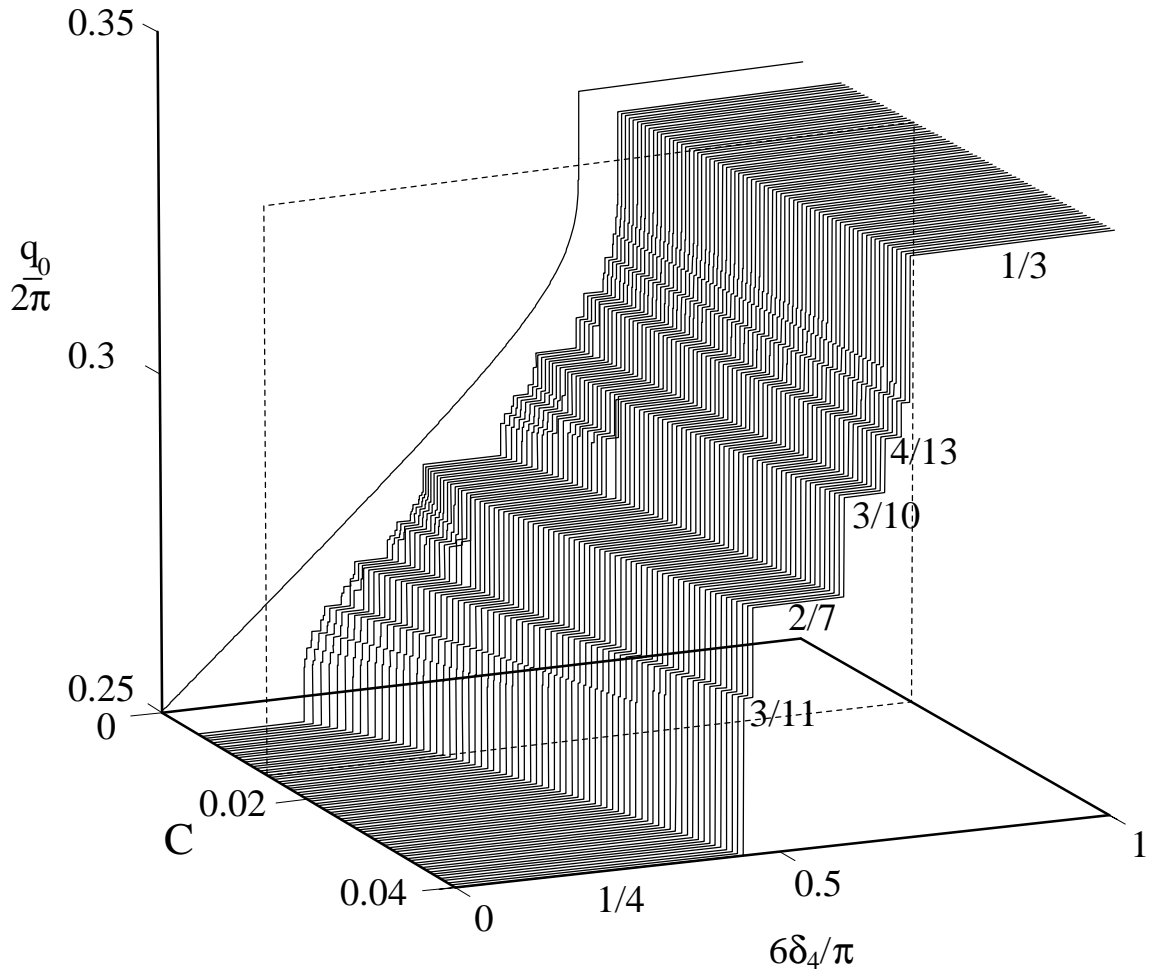


Fig. 9

